JACS
JOURNAL OF THE AMERICAN CHEMICAL SOCIETY
Article
pubs.acs.org/JACS

Phenyl Esters Are Potent Inhibitors of Caseinolytic Protease P and Reveal a Stereogenic Switch for Deoligomerization

Mathias W. Hackl,[†,#] Markus Lakemeyer,[†,#] Maria Dahmen,[†] Manuel Glaser,[‡] Axel Pahl,[†] Katrin Lorenz-Baath,[†] Thomas Menzel,[†] Sonja Sievers,[§] Thomas Böttcher,[⊥] Iris Antes,[‡] Herbert Waldmann,[§,∥] and Stephan A. Sieber*[,†]

[†]Center for Integrated Protein Science at the Department of Chemistry, Technische Universität München, Lichtenbergstrasse 4, Garching, D-85747, Germany

[‡]Center for Integrated Protein Science at the Department of Life Sciences, Technische Universität München, Emil-Erlenmeyer-Forum 8, D-85354 Freising, Germany

[§]Max-Planck-Institut für Molekulare Physiologie, Abteilung Chemische Biologie, Otto-Hahn-Strasse 11, D-44227 Dortmund, Germany

[∥]Technische Universität Dortmund, Fakultät für Chemie und Chemische Biologie, Otto-Hahn-Strasse 6, D-44221 Dortmund, Germany

[⊥]Department of Chemistry, Universität Konstanz, Universitätsstrasse 10, D-78457 Konstanz, Germany

Supporting Information

ABSTRACT: Caseinolytic protease P (ClpP) represents a central bacterial degradation machinery that is involved in cell homeostasis and pathogenicity. The functional role of ClpP has been studied by genetic knockouts and through the use of *beta*-lactones, which remain the only specific inhibitors of ClpP discovered to date. *Beta*-lactones have served as chemical tools to manipulate ClpP in several organisms; however, their potency, selectivity and stability is limited. Despite detailed structural insights into the composition and conformational flexibility of the ClpP active site, no rational efforts to design specific non-*beta*-lactone inhibitors have been reported to date. In this work, an unbiased screen of more than 137 000 compounds was used to identify five phenyl ester compounds as highly potent ClpP inhibitors that were selective for bacterial, but not human ClpP. The potency of phenyl esters largely exceeded that of *beta*-lactones in ClpP peptidase and protease inhibition assays and displayed unique target selectivity in living *S. aureus* cells. Analytical studies revealed that while phenyl esters are cleaved like native peptide substrates, they remain covalently trapped as acyl-enzyme intermediates in the active site. The synthesis of 36 derivatives and subsequent structure−activity relationship (SAR) studies provided insights into conserved structural elements that are important for inhibition potency and acylation reactivity. Moreover, the stereochemistry of a methyl-substituent at the *alpha* position to the ester, resembling amino acid side chains in peptide substrates, impacted ClpP complex stability, causing either dissociation into heptamers or retention of the tetradecameric state. Mechanistic insights into this intriguing stereo switch and the phenyl ester binding mode were obtained by molecular docking experiments.

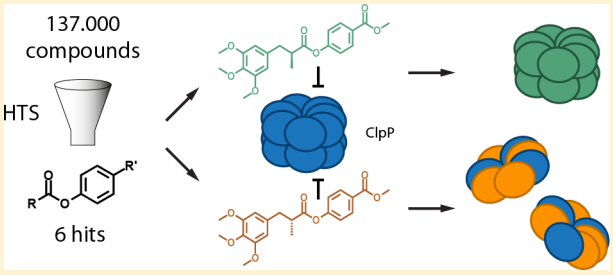

INTRODUCTION

Proteolysis represents an essential physiological mechanism for diverse cellular functions including post-translational processing, signaling and protein degradation.[1,2] This important process is catalyzed by a variety of proteases, which together constitute one of the largest enzyme classes in eukaryotic and prokaryotic cells. In prokaryotes, a variety of ATP-dependent proteases are responsible for protein degradation, including FtsH,[3] Lon[4] and HslUV.[5−7] One additional member of this group is the caseinolytic protease P (ClpP), a tetradecameric, barrel-shaped serine protease that associates with AAA+ chaperones such as ClpA, ClpC and ClpX for protein degradation.[8−13] The chaperones recognize, unfold and direct SsrA-tagged protein substrates into the proteolytic chamber of ClpP in an ATP-dependent manner.[14] ClpP is essential for the regulation of the cellular stress response, cell homeostasis and bacterial virulence.[10,15,16] Virulence, i.e., the expression of bacterial toxins such as *alpha*-hemolysin, is regulated by the Agr signaling network wherein ClpP is believed to be involved in the degradation of Rot, a repressor of bacterial toxins.[17] Genetic ClpP knockouts in *Listeria monocytogenes* and *Staphylococcus aureus* revealed a reduction in virulence, resulting in attenuated infections in murine abscess models.[10,18] Similarly, the same phenotype was observed upon the chemical inhibition of ClpP with long-chain aliphatic *beta*-lactones (e.g., **D3**, Figure 1B), the

Received: March 24, 2015
Published: June 17, 2015

DOI: 10.1021/jacs.5b03084
J. Am. Chem. Soc. 2015, 137, 8475−8483

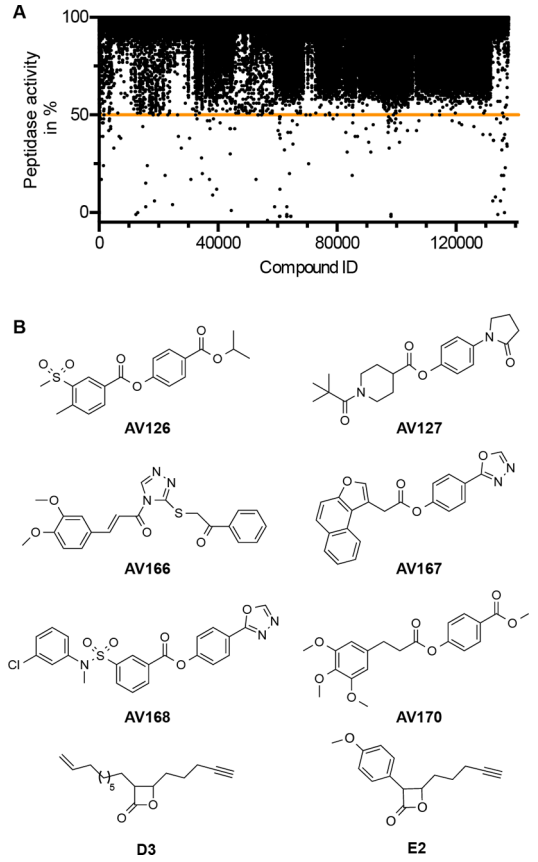

Figure 1. Identification of HTS primary hits. (A) A screen of more than 137 000 compounds identified 161 primary hits which reduced turnover of the fluorogenic substrate *N*-succinyl-Leu-Tyr-7-amido-4-methylcoumarin (SLY-AMC) by 50% at 12.5 μM concentration. (B) Structures of the six final hits that had suitable pharmacological properties and showed an IC_{50} < 2 μM, and structures of *beta*-lactone compounds **D3** and **E2**.

only specific inhibitors reported for ClpP to date.[19−21] Crystal structures of *S. aureus* ClpP revealed a deep hydrophobic channel next to the active site Ser98, which accommodates lactone side chains of maximum 8 atoms length.[22−24] Ser98 nucleophilically attacks the 4-membered lactone ring resulting in a covalent acyl-enzyme intermediate. Depending on the *beta*-lactone C-4 substitution, the occupancy of ClpP varies from stoichiometric for aliphatic **D3** to 50% for aromatic **E2**.[25] One reason for these differing ratios is the transient stability of the ClpP tetradecamer, which dissociates into heptamers via an unknown mechanism upon **E2** binding.

The interaction of subunits in the tetradecameric complex is facilitated by a dynamic H-bond network of adjacent helices (E-helix), *beta*-sheets (Gly-rich loop) and oligomerization sensors (Asp170-Arg171).[22] The E-helices exist in extended, compact and compressed conformations. While an extended helix supports an aligned and active catalytic triad (Ser98, His123 and Asp172), the compressed helix induces a rotation of the active site His123 and displaces the catalytic residues.[26] Moreover, in the compressed state all crucial interactions between the rings are abrogated leading to the formation of inactive heptamers. From a pharmacological perspective, inhibitor-induced heptamerization is advantageous as the corresponding enzyme, although not quantitatively acylated, is misaligned and inactive in all catalytic centers, effectively maximizing the sustainability of deactivation. Thus, drug discovery efforts for ClpP and other multimeric enzymes need to consider deoligomerization as an attractive mode of action.

As *beta*-lactones are labile electrophiles which quickly hydrolyze in human plasma within minutes,[19] previous rational attempts focused on replacing this group with more stable moieties. However, installation of lactam, carbamate, ester and oxetane moieties failed to inhibit the enzyme suggesting a restricted active site tolerance.[23] In order to expand the repertoire of ClpP inhibitors as chemical biology tools and to identify novel pharmacological leads we performed an unbiased high-throughput screen (HTS) of more than 137 000 compounds and identified six compounds as potent hits, which all contained activated ester or amide moieties. In-depth biochemical characterization and structure−activity relationship (SAR) studies revealed a new class of deoligomerizing ClpP inhibitors with superior potency, inhibition kinetics, plasma half-life, stability of the acyl-enzyme intermediate and specificity. The (*R*)- or (*S*)-configuration of a methyl substituent in the *alpha* position to the ester served as a switch of the oligomeric state which was further supported by molecular docking experiments.

RESULTS

High Throughput Screen for ClpP Inhibitors. For the discovery of novel, non-*beta*-lactone inhibitors of ClpP, we performed a HTS with more than 137 000 compounds, which were each tested for inhibition of *S. aureus* ClpP (SaClpP) peptidase activity. Compounds that inhibited turnover of the fluorogenic substrate *N*-succinyl-Leu-Tyr-7-amido-4-methylcoumarin (SLY-AMC) by 50% at 12.5 μM concentration were regarded as a hit. Dose−response behavior of the assay was validated using the ClpP inhibitor Palmostatin M, a *beta*-lactone, as a positive control (Figure S1). The overall Z′ factor of the primary screen was calculated to be 0.69 ± 0.14 and the overall signal-to-background ratio was 25 ± 9.

161 initial hits were identified (hit rate 0.017%) and their individual IC_{50} values determined (Figure 1A, Table S2). Compounds with an IC_{50} < 2 μM and desirable pharmacological properties (see Supporting Information for details on filtering criteria) were selected for further studies. Given the large number of molecules screened, it is surprising that only six hits met these criteria, demonstrating a restricted structural access to the ClpP active site (Figure 1B, Table S1). Interestingly, five molecules contained a central phenyl ester (of respective aromatic acids: **AV126**, **AV168** or aliphatic acids: **AV127**, **AV167**, **AV170**) and one compound a triazole amide motif (**AV166**). All compounds exhibited potent IC_{50} values between 0.3 and 1.3 μM which are even at the lower limit of the assay (requires 1 μM ClpP).

Although previous attempts to replace the lactone scaffold with open-chain esters and carbamates failed,[23] phenyl esters and triazole amides exhibit a stabilized aromatic leaving group that elevates electrophilicity, and thereby reactivity, toward Ser98. Remarkably, of the 1780 phenyl esters present in the library only five (0.3%) were identified as hits, emphasizing that not only reactivity, but also structural prerequisites, are important for binding and inhibition.

Customized Inhibitors of Bacterial and Human ClpP Peptidase and Protease Activity. The panel of inhibitors was tested for potency and selectivity against *S. aureus*, *Escherichia coli*, *L. monocytogenes* and human ClpP. First, inhibition of ClpP-catalyzed SLY-AMC peptide hydrolysis was

DOI: 10.1021/jacs.5b03084
J. Am. Chem. Soc. 2015, 137, 8475−8483

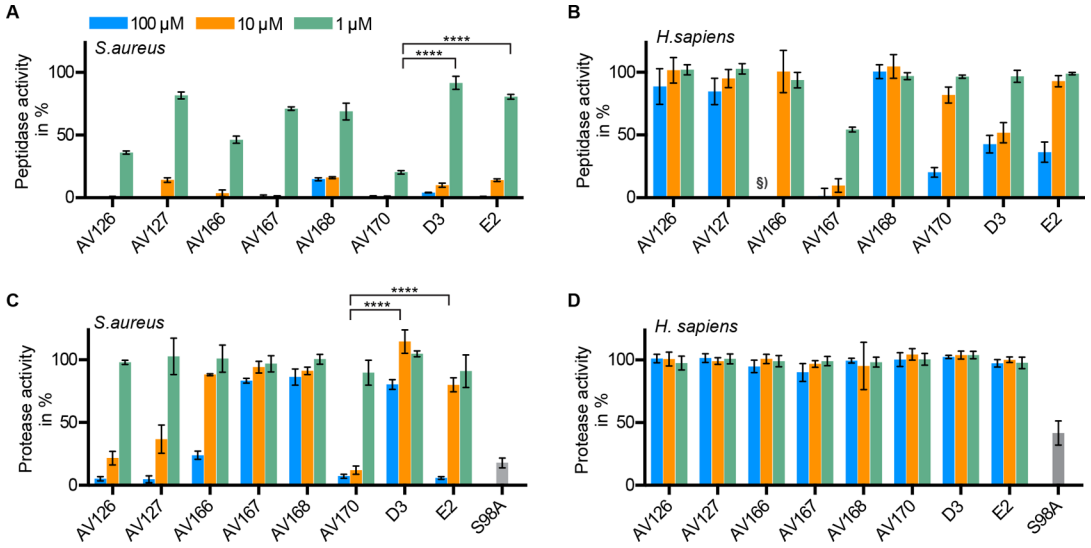

Figure 2. Inhibition of ClpP peptidase and ClpXP protease activity. Hit compounds and two lactone inhibitors (**E2** and **D3**) were tested at three concentrations for their inhibition of peptidase and protease activity. Data are normalized with respect to DMSO as a negative control (100% activity) (A) *S. aureus* ClpP peptidase assay (1 μM SaClpP in the presence of 200 μM SLY-AMC) (B) *H. sapiens* ClpP peptidase assay (1 μM HsClpP in the presence of 200 μM SLY-AMC). (C) *S. aureus* ClpP protease assay (0.2 μM SaClpP in the presence of 0.4 μM SaClpX and 0.4 μM GFP-SsrA) (D) *H. sapiens* ClpP protease assay (0.2 μM HsClpP in the presence of 0.4 μM EcClpX[#] and 0.4 μM GFP-SsrA). Each data set represents six replicates obtained from two independent experiments (mean ± standard deviation). **** represent *p*-value ≤0.0001 determined by Student's *t* test. [#]EcClpX was used in place of HsClpX as the AAA+ Chaperone to recognize, unfold and translocate the substrate as described previously.[28] [§]Internal fluorescence of compound **AV166** precluded measurements at 100 μM.

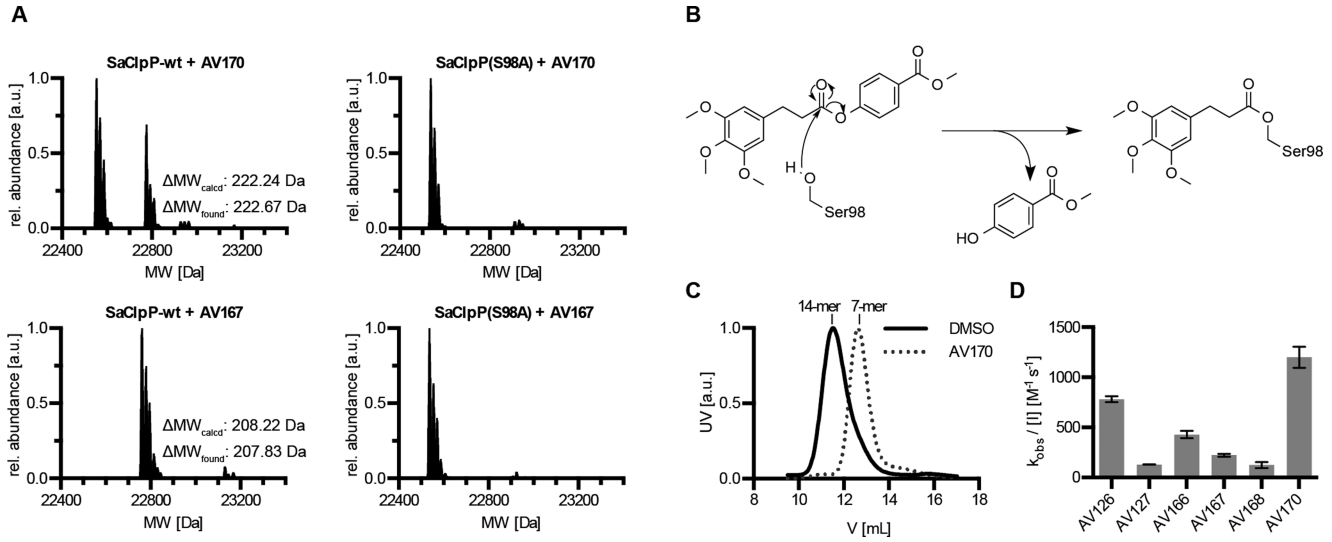

Figure 3. Phenyl esters covalently modify ClpP. (A) Intact protein mass spectrometry of SaClpP after compound treatment reveals incomplete (**AV170**) and full (**AV167**) modification whereas the respective active site mutant SaClpP(S98A) lacks binding. (B) Suggested mode of action, illustrated for **AV170**. (C) Size-exclusion chromatograms show SaClpP heptamer formation upon treatment with **AV170**. (D) SaClpP inactivation rates (k_{obs}/[I] values) for the six hit compounds.

determined by the percent residual activity at 100, 10, and 1 μM compound concentration across the panel of enzymes. In prokaryotic ClpP, **AV170** exhibited the most pronounced reduction in peptide hydrolysis followed by **AV166** and **AV126** (Figure 2A and Figure S2). Importantly, at the lowest concentration tested (1 μM), **AV170** was four times more effective (for SaClpP) compared to the previously reported *beta*-lactone inhibitors **D3** and **E2,** which have served as a gold standard for ClpP inhibition so far.[21] On the contrary, the best inhibitors of bacterial ClpP did not significantly reduce human ClpP (hClpP) peptidase activity even at low to moderate (1 to 10 μM) concentrations, pointing toward significant differences in the binding sites (Figure 2B). Human and *S. aureus* ClpP share only a moderate sequence similarity of 37%. Since the inactivation of human ClpP has been linked to cancer and the *Perrault* syndrome[27] the observed discrimination between human and bacterial enzymes is beneficial for putative medicinal applications. In turn, **AV167**, with a large naphthofuran moiety, was the only compound that significantly reduced human ClpP peptidase activity even at low (1 μM) concentrations (Figure 2B).

To examine if the identified peptidase inhibitors also impair proteolysis, we monitored the digest of green fluorescent protein (GFP) tagged with a SsrA peptide sequence. Bacterial

DOI: 10.1021/jacs.5b03084
J. Am. Chem. Soc. 2015, 137, 8475−8483

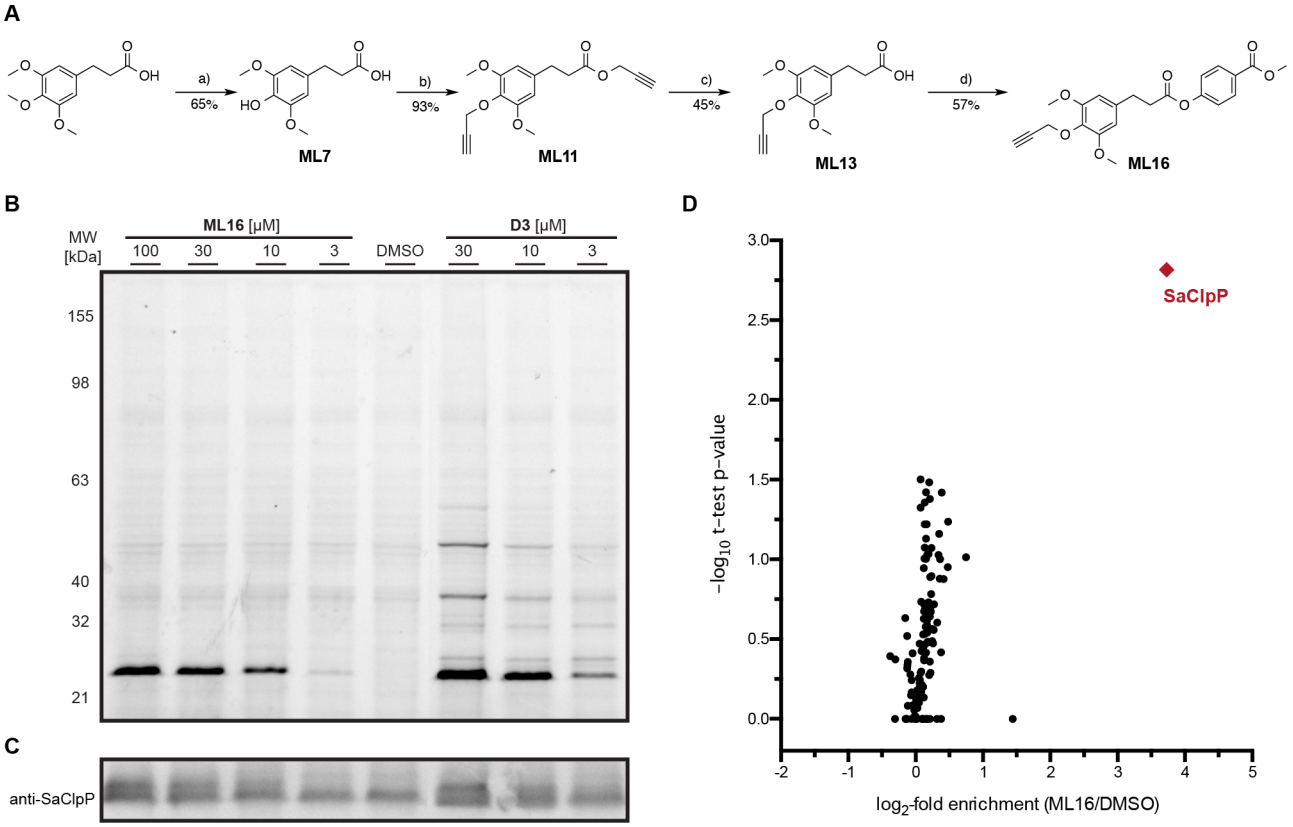

Figure 4. Synthesis of **ML16** and in situ target analysis. (A) Scheme for the synthesis of activity-based probe **ML16**. Reagents and conditions: (a) MgI_2, *neat*, 80 °C, 1.5 h; (b) propargyl bromide, K_2CO_3, KO^{t}Bu, DMF, rt, 72 h; (c) 15% aq. NaOH, MeOH, 50 °C, 2 h; (d) methyl 4-hydroxybenzoate, EDC·HCl, DMAP, DCM, rt, 24 h. (B,C) ABPP-labeling of living *S. aureus* cells with **ML16** and **D3**. (B) Fluorescence SDS-PAGE of soluble fraction. (C) Western blot against SaClpP confirming the labeling of ClpP. See Figure S7 for full image and overlay of Western blot and fluorescence scan. Note: Probe binding slightly changes protein migration explaining the double band in Western Blots of treated samples. (D) Vulcano plot representation of gel-free quantitative ABPP experiments with **ML16**. ClpP is identified as the only target of **ML16** (13-fold enrichment over DMSO, *p*-value of 0.0015). Data are derived from three independent experiments.

ClpX recognizes SsrA as a degradation signal, unfolds, and subsequently directs the protein into the ClpP proteolytic chamber.[14,29] Proteolytic activity of the SaClpXP complex was effectively inhibited at 10 μM by phenyl esters **AV126** and **AV170** which is nearly 11-fold more potent compared to the lactones **D3** and **E2** (Figure 2C). In line with previous reports,[29] the proteolytically inactive ClpXP(S98A) complex reduced GFP fluorescence solely by ClpX-mediated unfolding (about 17%). However, no reduction of fluorescence was observed in ClpXP samples treated with phenyl esters, suggesting that compounds not only abolished GFP degradation but also impaired its unfolding. None of the phenyl ester compounds inhibited human ClpXP proteolysis, demonstrating the desired selectivity for bacterial ClpP species (Figure 2D).

Phenyl Esters Covalently Bind to the Active Site and Induce ClpP Deoligomerization. Given the compelling activity of phenyl esters in peptidase and protease assays, we next focused on elucidating the mechanism of inhibition of SaClpP as the biologically relevant target. Phenyl esters and triazole amides represent electrophilic molecules that can inhibit ClpP by either covalent or noncovalent binding. In order to investigate the binding mode and the degree of modification, we utilized intact protein mass spectrometry and determined the exact mass of SaClpP treated with inhibitor. All compounds active in *S. aureus* peptidase assays shifted the protein mass to higher molecular weights, confirming a covalent binding mechanism (Figure 3A, Figure S3). The extent of modification ranged from 25% for **AV168** to 50% for **AV170**. Only the human ClpP inhibitor **AV167** achieved binding saturation (Figure 3A). None of the molecules were able to bind the SaClpP(S98A) mutant, reaffirming the role of active site Ser98 as the functional nucleophile (Figure 3A, Figure S3).

Moreover, the adduct mass corresponded to the attachment of only the carboxy part of the esters. These findings elucidate a mode of inhibition in which the inhibitor binds to the active site, undergoes nucleophilic attack by Ser98 at the ester or amide and releases the phenol or triazole as a stabilized leaving group (Figure 3B). Activated ester inhibitors thus act as substrate mimics which are cleaved like native peptides but remain trapped in the acyl-enzyme intermediate state.

Previous studies with *beta*-lactones **D3** and **E2** showed that binding to the active site of ClpP can either result in acylation of all sites (**D3**) under retention of the oligomeric state, or in partial modification and subsequent deoligomerization (**E2**).[25] Here, all phenyl esters and triazole amides followed the deoligomerization route leading to inactive heptamers (Figure 3C, Figure S4). This conformational change disassembles the ClpP barrel, stalls proteins at ClpX, and thus explains the surprising dual inhibition of unfolding and degradation activity with **AV170** and **AV126**.

In order to determine the potency of the covalent phenyl ester and triazole amide inhibitors, we measured the inactivation rates via $k_{obs}/[I]$ values. The highest $k_{obs}/[I]$ values, i.e., acylation velocities, were obtained with **AV170**

DOI: 10.1021/jacs.5b03084
J. Am. Chem. Soc. 2015, 137, 8475−8483

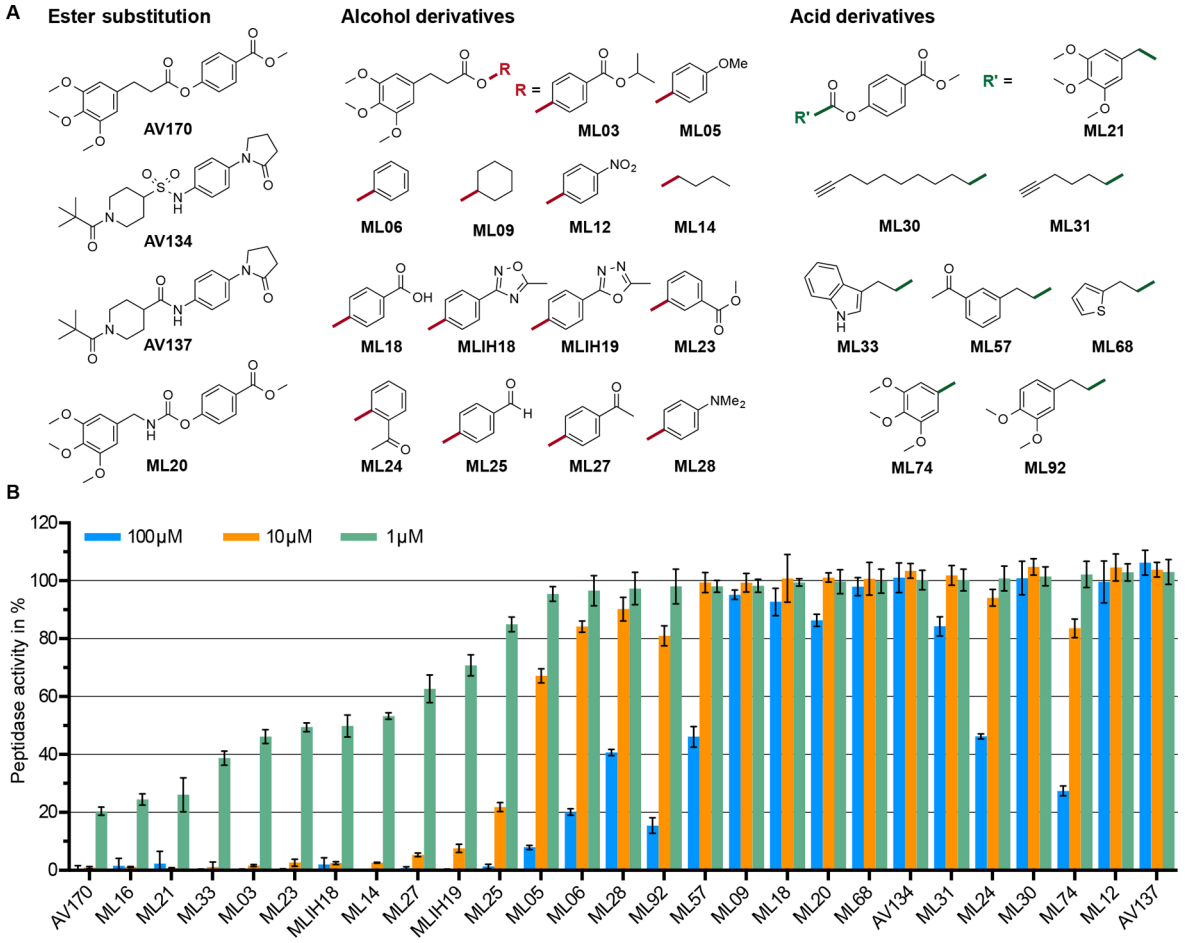

Figure 5. Structure–activity relationship studies. (A) Chemical structures of **AV170** and its synthesized derivatives modified at the ester, alcohol or acid moiety. (B) Inhibition of SaClpP peptidase activity by the compounds. Each data set represents six replicates from two independent experiments (mean ± standard deviation).

(1200 ± 105 M^{-1} s^{-1}) and **AV126** (781 ± 31 M^{-1} s^{-1}). This accounts for approximately 20 times faster reaction kinetics in the case of **AV170**, compared to the previous gold standard inhibitors **D3** (78 ± 6 M^{-1} s^{-1}) and **E2** (64 ± 3 M^{-1} s^{-1}) (Figure 3D, Figure S5).[25] On the basis of its superior activity, **AV170** was selected as the most promising candidate for in situ target validation.

ClpP Is the Predominant Intracellular Target of Phenyl Esters in *S. aureus*. Prior to compound optimization, cell permeability and target selectivity of **AV170** in living *S. aureus* cells were analyzed. We utilized a chemical proteomic strategy termed activity-based protein profiling (ABPP)[30,31] wherein we synthesized an alkyne-tagged **AV170** derivative which remains bound to the enzyme upon inhibition. The alkyne serves as a benign tag for subsequent conjugation to a functionalized azide via the Huisgen–Sharpless–Meldal cycloaddition (click chemistry).[32−34] In brief, the synthesis started with 3-(3,4,5-trimethoxyphenyl)propanoic acid which was selectively demethylated in the *para* position by means of magnesium iodide (Figure 4A).[35] Global propargylation and ester hydrolysis, followed by esterification with methyl-4-hydroxybenzoate yielded the final probe **ML16**. The compound showed similar potency in SaClpP peptidase inhibition compared to **AV170** (Figure 5B) and intact protein mass spectrometry confirmed covalent modification of the enzyme with about 22% (Figure S6). The probe was incubated with intact *S. aureus* cells for 1h, followed by cell lysis, proteome separation into soluble and insoluble fractions, treatment with a rhodamine azide dye, separation on SDS-PAGE and visualization via fluorescent scanning. Importantly, only a single band appeared on the fluorescent SDS gel, which could be identified as ClpP by Western blotting, (Figure 4B, C, Figure S7 for entire blot). The lack of any off-targets surpassed the selectivity of **D3**, which weakly labeled additional bands, and thereby establishes phenyl esters as selective ClpP inhibitors. Furthermore, the ClpP band in **D3** treated samples could selectively be outcompeted by **AV170** while all off-targets of **D3** remained unchanged (Figure S8). Quantitative MS-based proteomic experiments further underlined the unprecedented selectivity of **ML16** for ClpP as the predominant target in living *S. aureus* cells (Figure 4D). ClpP was the only identified target and was enriched about 13-times over the DMSO control with a *p*-value of 0.0015 (see Supporting Information for further experimental details).

Structure–Activity Relationship Studies. To explore the SAR of phenyl esters, we systematically varied the phenol group, the carboxylic acid moiety and the ester bond of **AV170** and **AV127** (Figure 5A, Scheme S1–S3). Substitution of the ester bond by carbamates (**ML20**), amides (**AV137**) or sulfonamides (**AV134**) led to inactive compounds (Figure 5B). Therefore, the ester was kept as an integral part of this inhibitor class. The phenol of **AV170** is substituted with an

DOI: 10.1021/jacs.5b03084
J. Am. Chem. Soc. 2015, 137, 8475–8483

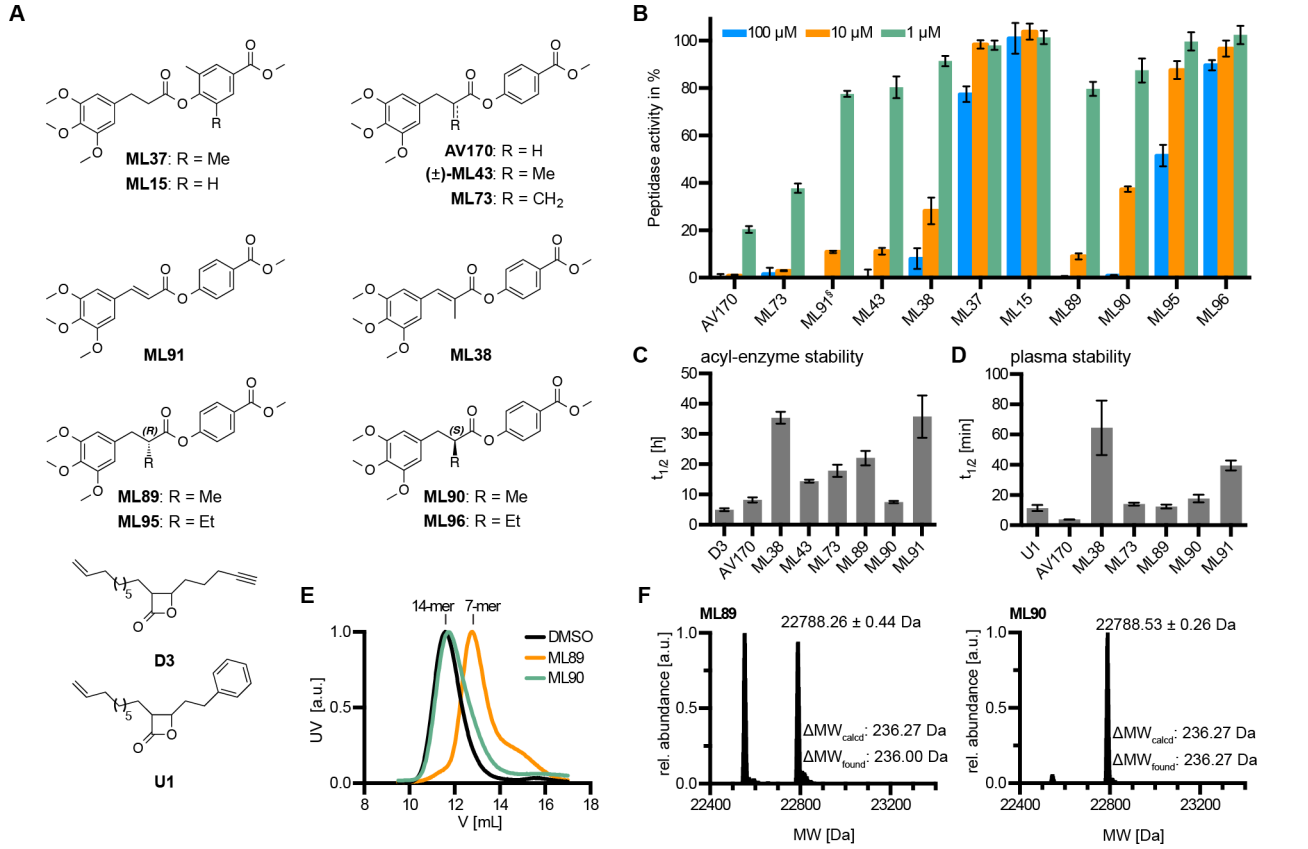

Figure 6. (A) Chemical structures of stabilized **AV170** derivatives. (B) Inhibition of peptidase activity upon treatment with respective compounds. Each data set represents six replicates from two independent experiments (mean ± standard deviation). (C) Stability of various acyl-SaClpP complexes at 32 °C as determined by time-dependent intact protein mass spectrometry. Half life refers to the time needed for a 50% reduction in the extent of protein modification (see Figure S9 for raw data). Each data set represents three biological replicates (mean ± standard deviation). (D) Compound stability in human blood plasma. Each data set represents three independent experiments (mean ± standard deviation). (E) Size-exclusion chromatograms illustrating heptamer formation upon treatment with the (*R*)-enantiomer **ML89**. (F) Intact protein mass spectrometry showing partial (**ML89**) and full (**ML90**) modification of SaClpP after compound treatment. §Internal fluorescence of compound **ML91** precluded measurements at 100 μM.

electron-withdrawing group in the *para* position, which increases its lability. Interestingly, all HTS hits contained electron-withdrawing phenol substituents such esters (**AV126**, **AV170**), lactams (**AV127**) or oxadiazoles (**AV167**, **AV168**), suggesting that this electronic fine-tuning is a substantial driving force for reactivity and ClpP acylation. Accordingly, removal of the electron-withdrawing group (**ML06**) or exchange to electron donating groups such as methoxy (**ML05**) and *N*′,*N*′-dimethylamine (**ML28**) resulted in a significant drop in potency (Figure 5B). In addition, an ester derivative of cyclohexanol (**ML09**) exhibited no activity. We thus increased the diversity of electron-withdrawing substituents and altered their position on the phenol ring. Aldehydes (**ML25**), ketones (**ML27**) and isopropylesters (**ML03**) in the *para* position were among the best inhibitors (Figure 5B). While the ester group was tolerated in the *meta* postion (**ML23**), a keto-group in the *ortho* position (**ML24**) displayed almost no activity, suggesting that electronic and steric restrictions in the active site alter inhibitor potency. This is also supported by the observation that electron-withdrawing *p*-nitro (**ML12**) and *p*-carboxy (**ML18**) substituents were inactive, while the small, non-activated aliphatic butanol ester (**ML14**) retained moderate inhibitory activity.

Next, we explored the carboxylic acid moiety of **AV170** and determined a very limited structural flexibility in this part of the molecule. Variations of aromatic substituents (**ML92**, **ML57**) and replacement of the benzene ring by aliphatic residues (**ML30** and **ML31**) were not tolerated for ClpP inhibition. Interestingly, **ML33**, bearing an indole moiety, was among the best inhibitors while **ML68**, with an aromatic thiophene, displayed no potency (Figure 5B).

In **AV170**, the trimethoxyphenyl moiety and the reactive ester are separated by two methylene groups. We successively removed both methylene groups to generate compounds **ML21** and **ML74**. While **ML21** was active, **ML74** displayed only weak activity compared to **AV170**, suggesting that chain length is a crucial parameter for activity.

Chemical Modifications Increase Stability and Reveal a ClpP Deoligomerization Switch. *Beta*-lactones exhibit limited stability in acyl-enzyme complexes. Interestingly, the half-life of the **AV170** acyl-enzyme intermediate was higher compared to the respective **D3** acyl-enzyme complex ($t_{1/2}$ = 8.2 ± 0.8 h vs $t_{1/2}$ = 5.0 ± 0.4 h) (Figure 6C, Figure S9). To improve compound stability, we rationalized that substituents *alpha* to the carbonyl could sterically hinder hydrolysis. We therefore synthesized derivatives of **AV170** containing either methyl (**ML38**, **ML43**, **ML89**, **ML90**), methylene (**ML73**) or ethyl substituents (**ML95**, **ML96**) at this position (Figure 6A). Moreover, methyl groups were installed in the *ortho* position of the phenol ring (**ML15**, **ML37**) to protect the ester from the

DOI: 10.1021/jacs.5b03084
J. Am. Chem. Soc. 2015, 137, 8475−8483

opposite side (Figure 6A). While incorporation of methyl groups in the phenyl ring abolished inhibitor activity, methylation at the *alpha* position (**ML43**, **ML89**, **ML90**) enhanced acyl-enzyme stability with a moderate reduction of potency compared to **AV170** (Figure 6B,C). **ML73**, containing a methylene substituent, was the most potent compound in this series and also showed an improved half-life. Extended conjugated systems (**ML38**, **ML91**), leading to mesomeric stabilization, exhibited the most prominent prolongation of acyl-enzyme half lifes. Similar trends were observed for compound stability in human blood plasma (Figure 6D, Figure S10). Mesomeric stabilization by the extended conjugated system exhibited the best stabilizing effects (**ML38**, **ML91**) with half lifes of up to 65 ± 18 h. This corresponds to a 20-fold and 6-fold improvement compared to **AV170** (3.7 ± 0.1 h) and *beta* lactone **U1** (11 ± 2 h),[19] respectively. Sterical shielding of the carbonyl via introduction of a methyl (**ML89**, **ML90**) or methylene group (**ML73**) had a less pronounced influence on stabilization.

ML43 was initially tested as a racemic mixture. To discriminate between the properties of each enantiomer, we stereoselectively synthesized both (*S*)-**ML90** and (*R*)-**ML89** using a chiral auxiliary (Figure 6A, Scheme S4, S5). (*R*)-**ML89** is moderately more potent than (*S*)-**ML90** (Figure 6B) and exhibited 3-fold enhanced acyl-enzyme stability (Figure 6C). In agreement with the mode of action of other phenyl esters, (*R*)-**ML89** partially modified ClpP and induced dissociation into heptamers (Figure 6E,F). Surprisingly, unlike all other phenyl esters studied so far, the orientation of the methyl group in (*S*)-**ML90** resulted in acylation of all 14 ClpP active sites and retention of the tetradecameric assembly (Figure 6E,F). It is an intriguing feature of these inhibitors that the orientation of the methyl substituent acts as a switch that either stabilizes or destabilizes the transient ClpP complex. Contrastingly, an ethyl group at this position ((*R*)-**ML95** and (*S*)-**ML96**) abolished activity, demonstrating that longer chains are not tolerated (Figure 6B).

As ClpP activity is important for bacterial virulence the inhibitors were tested in a hemolysis assay. A reduction in hemolysis was observed with compounds **AV170**, **ML21**, **ML89** and **ML90** through dose−response curves, with EC_{50} values ranging from 60−200 μM (Figure S11). However, upon prolonged incubation of bacterial supernatants with red blood cells, residual hemolytic activity could be detected, suggesting that *alpha*-hemolysin production was not completely attenuated. No cytotoxic effects were observed at a concentration of 100 μM for **AV170**, **ML21**, **ML89** and **ML90** (Figure S12) against human epithelial lung cancer cells A549. This is in line with in situ labeling experiments which showed weak labeling of only two distinct bands in the soluble protein fraction of A549 cells upon incubation with the phenyl ester probe **ML16** (Figure S13).

Molecular Docking Reveals the Binding Mode of Phenyl Esters. To elucidate the binding mode of phenyl esters to ClpP in more detail and to investigate the underlying cause of the (*R*),(*S*)-enantiomer switch, we completed molecular docking studies with compounds **AV170**, **ML21**, **ML89**, **ML90**, and nonbinding **ML74**. The docking solutions were filtered using pharmacophoric constraints to ensure the correct placement of the carbonyl oxygen in the oxyanion hole, which is a prerequisite for the nucleophilic attack to occur. Molecular dynamics (MD) simulations were subsequently performed for the three best poses of each compound. Figure 7 illustrates the most energetically favored conformations upon MD refinement. All inhibitors show the same general binding mode, as exemplified by **AV170** in Figure 7A. The trimethoxyphenyl moiety of **AV170** binds to a distinct hydrophobic channel extending from the catalytic center, while the reactive ester points toward the oxyanion hole (red circle).

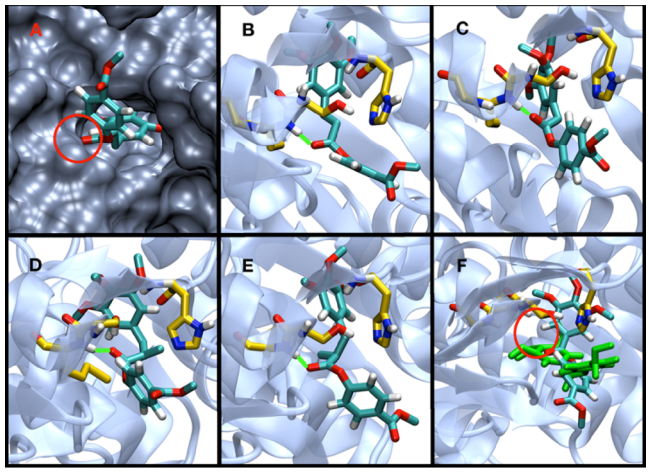

Figure 7. (A) Surface representation of the ClpP active site bound to **AV170**. (B−F) Conformations of five selected compounds after MD refinement. Important residues of the catalytic site and the oxyanion hole (M99, S98, H123), as well as bound ligands are shown in stick representation. (B) **AV170**. (C) **ML21**. (D) **ML89**. (E) **ML90**. (F) **ML74**. Final conformations of **ML74** are given in green.

Previous mutation experiments have validated this pocket as an integral part of the binding mode of *beta*-lactones.[23] Here, mutation of Leu154 to Tyr restricted the pocket size and strongly reduced binding of **AV170**, while the shorter **ML21** derivative was unaffected (Figure S14). We calculated the equilibrated bound structures of **AV170** as well as **ML21** and **ML74** within this binding pocket. In order to fully accommodate the trimethoxyphenyl moiety, a flexible linker is needed to span the constricted area between the catalytic center and the hydrophobic pocket. In the case of **AV170**, the two-carbon linker appears to have an optimal length to accommodate the trimethoxyphenyl ring. In **ML21**, the methylene linker still allows the ring to enter the pocket but its conformation is more constricted, whereas **ML74**, with its shorter linker, places the bulky trimethoxyphenyl ring directly at the pocket entrance and prohibits a stable conformation where the reactive ester group is close enough to the oxyanion hole for the reaction to occur (Figure 7F). Moreover, no hydrogen bond between the backbone amino group of the oxyanion hole and the ester groups of **ML74** is formed. This leads to the release of compound out of the pocket during MD (final conformation given in green) for all three investigated poses, whereas all three poses of **AV170** and **ML21** remained in their bound conformation (Figure 7B−E).

Next, we looked into the strikingly different binding and deoligomerization behaviors of compounds **ML89** and **ML90** (Figure 7D,E). A comparison of these compounds with **AV170** (same linker length, but no methyl group) revealed two main differences. First, the methyl group of **ML89**/**ML90** strongly restricts possible binding conformations as it is located directly at the constricted area between the catalytic center and the hydrophobic binding pocket. Second, the relative orientation of the methyl group largely diverges in the two stereoisomers. In

DOI: 10.1021/jacs.5b03084
J. Am. Chem. Soc. 2015, 137, 8475−8483

ML90, the methyl group is located at the bottom of the constricted area. In the case of the **ML89** stereoisomer, the methyl group points to the top of the binding site toward the histidine of the catalytic triad. As there is more space in this direction, there seem to be less conformational restrictions compared to **ML90**. Importantly, this histidine has previously been identified as part of a hydrogen bonding network which plays a crucial role for the deoligomerization process.[26] Thus, the relative orientation of the inhibitor scaffold of **ML89** compared to **ML90** may trigger a steric rearrangement which causes the observed deoligomerization.

DISCUSSION

Functional and mechanistic analysis of the ClpXP proteolytic system represents an area of intense research. Recent reports have focused on mechanistic aspects of the whole ClpXP unfolding machinery.[36−38] *Beta*-lactones, the only specific ClpP inhibitors reported to date, have been applied as tools to probe the binding pocket and mechanism of inhibition, as well as the transient stability of the ClpP tetradecamer and its conformational switching.[23,25,39] One additional consequence of *beta*-lactone-based ClpP inhibition is the reduction of virulence in pathogenic bacteria such as MRSA and the eradication of *Mycobacteria* that express two essential ClpP isoforms.[19,20,40] Here, we expand the set of ClpP tools through a novel class of phenyl esters that surpass *beta*-lactones in terms of potency in peptidase and protease inhibition, reaction kinetics, target selectivity in the soluble fraction of the proteome, plasma half-life, acyl-enzyme stability and deoligomerization as the preferred mechanism of inhibition. Contrary to *beta*-lactones, phenyl esters closely mimic the natural peptide substrate in which the acyl-enzyme intermediate is irreversibly trapped and the phenol released. Our SAR studies showed that an electron-deficient phenol moiety is important in maintaining a level of reactivity that facilitates the attack of the active site serine. The ester must be substituted with an aromatic system that is linked via at least one methylene bridge in order to pass a constricted area in the binding pocket.

Importantly, introduction of a methyl group in the *alpha* position not only enhances the acyl-enzyme stability but also yields a switch that, depending on the absolute configuration, retains the oligomeric state or induces dissociation into heptamers. Considering that the native peptide backbone branches at the same position, it is intriguing to speculate that this inhibitor-trapped intermediate may reflect a transition of ClpP-mediated substrate turnover.

It is worth noting that the HTS only revealed a very limited set of potent inhibitors and that all of these utilize a covalent mode of action. These potent inhibitors help to elucidate and dissect ClpP action; however, their translation into pharmacologically suitable virulence blockers still represents a major challenge. Inspired by the marketed phenyl ester protease inhibitor sivelestat, protection of the ester group by adjacent methyl substituents increased the ester stability, at the cost of ClpP reactivity. Thus, future studies have to consider the two opposing factors, stability and reactivity, in order to identify an optimal pharmacological candidate.

ASSOCIATED CONTENT

Supporting Information

Additional text, figures, tables and schemes giving biochemical data, labeling results, synthetic strategies, compound characterization data and ^{1}H and ^{13}C NMR spectra. The Supporting Information is available free of charge on the ACS Publications website at DOI: 10.1021/jacs.5b03084.

AUTHOR INFORMATION

Corresponding Author

*stephan.sieber@tum.de

Author Contributions

#M.W.H. and M.L. contributed equally to this work.

Notes

The authors declare no competing financial interest.

ACKNOWLEDGMENTS

The work was funded by the Deutsche Forschungsgemeinschaft, SFB749, SFB1035, FOR1406 and the ERC starting grant (250924-antibacterials). We would like to acknowledge Eilika Weber-Ban (ETH Zürich) for generously providing the EcClpX plasmid. We thank Malte Gersch and Matthias Stahl for providing purified EcClpX, EcClpP and hClpP proteins, as well as Ines Hübner for support in the synthesis of compounds MLIH18 and MLIH19. Furthermore, we would like to acknowledge Ernst Bernges, Burghard Cordes and Mona Wolff for technical assistance, Elena Kunold for help with analysis of quantitative mass spectrometry data and Vadim Korotkov and Annabelle Hoegl for critical revision of the manuscript.

REFERENCES

(1) Ehrmann, M.; Clausen, T. *Annu. Rev. Genet.* **2004**, *38*, 709.
(2) Walsh, C. T.; Garneau-Tsodikova, S.; Gatto, G. J., Jr. *Angew. Chem., Int. Ed. Engl.* **2005**, *44*, 7342.
(3) Bieniossek, C.; Schalch, T.; Bumann, M.; Meister, M.; Meier, R.; Baumann, U. *Proc. Natl. Acad. Sci. U. S. A.* **2006**, *103*, 3066.
(4) Botos, I.; Melnikov, E. E.; Cherry, S.; Khalatova, A. G.; Rasulova, F. S.; Tropea, J. E.; Maurizi, M. R.; Rotanova, T. V.; Gustchina, A.; Wlodawer, A. *J. Struct. Biol.* **2004**, *146*, 113.
(5) Liu, K.; Ologbenla, A.; Houry, W. A. *Crit. Rev. Biochem. Mol. Biol.* **2014**, *49*, 400.
(6) Ramachandran, R.; Hartmann, C.; Song, H. K.; Huber, R.; Bochtler, M. *Proc. Natl. Acad. Sci. U. S. A.* **2002**, *99*, 7396.
(7) Bochtler, M.; Ditzel, L.; Groll, M.; Huber, R. *Proc. Natl. Acad. Sci. U. S. A.* **1997**, *94*, 6070.
(8) Baker, T. A.; Sauer, R. T. *Biochim. Biophys. Acta* **2012**, *1823*, 15.
(9) Katayama-Fujimura, Y.; Gottesman, S.; Maurizi, M. R. *J. Biol. Chem.* **1987**, *262*, 4477.
(10) Frees, D.; Qazi, S. N.; Hill, P. J.; Ingmer, H. *Mol. Microbiol.* **2003**, *48*, 1565.
(11) Thompson, M. W.; Maurizi, M. R. *J. Biol. Chem.* **1994**, *269*, 18201.
(12) Battesti, A.; Gottesman, S. *Curr. Opin. Microbiol.* **2013**, *16*, 140.
(13) Weber-Ban, E. U.; Reid, B. G.; Miranker, A. D.; Horwich, A. L. *Nature* **1999**, *401*, 90.
(14) Gottesman, S.; Roche, E.; Zhou, Y.; Sauer, R. T. *Genes Dev.* **1998**, *12*, 1338.
(15) Gaillot, O.; Pellegrini, E.; Bregenholt, S.; Nair, S.; Berche, P. *Mol. Microbiol.* **2000**, *35*, 1286.
(16) Frees, D.; Andersen, J. H.; Hemmingsen, L.; Koskenniemi, K.; Baek, K. T.; Muhammed, M. K.; Gudeta, D. D.; Nyman, T. A.; Sukura, A.; Varmanen, P.; Savijoki, K. *J. Proteome Res.* **2012**, *11*, 95.
(17) Frees, D.; Sorensen, K.; Ingmer, H. *Infect. Immun.* **2005**, *73*, 8100.
(18) Gaillot, O.; Bregenholt, S.; Jaubert, F.; Di Santo, J. P.; Berche, P. *Infect. Immun.* **2001**, *69*, 4938.
(19) Weinandy, F.; Lorenz-Baath, K.; Korotkov, V. S.; Böttcher, T.; Sethi, S.; Chakraborty, T.; Sieber, S. A. *ChemMedChem* **2014**, *9*, 710.
(20) Böttcher, T.; Sieber, S. A. *J. Am. Chem. Soc.* **2008**, *130*, 14400.

DOI: 10.1021/jacs.5b03084
J. Am. Chem. Soc. 2015, 137, 8475−8483

(21) Böttcher, T.; Sieber, S. A. *Angew. Chem., Int. Ed. Engl.* **2008**, *47*, 4600.
(22) Gersch, M.; List, A.; Groll, M.; Sieber, S. A. *J. Biol. Chem.* **2012**, *287*, 9484.
(23) Gersch, M.; Gut, F.; Korotkov, V. S.; Lehmann, J.; Böttcher, T.; Rusch, M.; Hedberg, C.; Waldmann, H.; Klebe, G.; Sieber, S. A. *Angew. Chem., Int. Ed. Engl.* **2013**, *52*, 3009.
(24) Geiger, S. R.; Böttcher, T.; Sieber, S. A.; Cramer, P. *Angew. Chem., Int. Ed. Engl.* **2011**, *50*, 5749.
(25) Gersch, M.; Kolb, R.; Alte, F.; Groll, M.; Sieber, S. A. *J. Am. Chem. Soc.* **2014**, *136*, 1360.
(26) Zeiler, E.; List, A.; Alte, F.; Gersch, M.; Wachtel, R.; Poreba, M.; Drag, M.; Groll, M.; Sieber, S. A. *Proc. Natl. Acad. Sci. U. S. A.* **2013**, *110*, 11302.
(27) Kang, S. G.; Ortega, J.; Singh, S. K.; Wang, N.; Huang, N. N.; Steven, A. C.; Maurizi, M. R. *J. Biol. Chem.* **2002**, *277*, 21095.
(28) Jenkinson, E. M.; Rehman, A. U.; Walsh, T.; Clayton-Smith, J.; Lee, K.; Morell, R. J.; Drummond, M. C.; Khan, S. N.; Naeem, M. A.; Rauf, B.; Billington, N.; Schultz, J. M.; Urquhart, J. E.; Lee, M. K.; Berry, A.; Hanley, N. A.; Mehta, S.; Cilliers, D.; Clayton, P. E.; Kingston, H.; Smith, M. J.; Warner, T. T.; University of Washington Center for Mendelian Genetics; Black, G. C.; Trump, D.; Davis, J. R.; Ahmad, W.; Leal, S. M.; Riazuddin, S.; King, M. C.; Friedman, T. B.; Newman, W. G. *Am. J. Hum. Genet.* **2013**, *92*, 605.
(29) Kim, Y. I.; Burton, R. E.; Burton, B. M.; Sauer, R. T.; Baker, T. A. *Mol. Cell* **2000**, *5*, 639.
(30) Evans, M. J.; Cravatt, B. F. *Chem. Rev.* **2006**, *106*, 3279.
(31) Fonovic, M.; Bogyo, M. *Curr. Pharm. Des.* **2007**, *13*, 253.
(32) Huisgen, R. *Proc. Chem. Soc.* **1961**, 357.
(33) Rostovtsev, V. V.; Green, J. G.; Fokin, V. V.; Sharpless, K. B. *Angew. Chem., Int. Ed. Engl.* **2002**, *41*, 2596.
(34) Tornøe, C. W.; Christensen, C.; Meldal, M. *J. Org. Chem.* **2002**, *67*, 3057.
(35) Bao, K.; Fan, A.; Dai, Y.; Zhang, L.; Zhang, W.; Cheng, M.; Yao, X. *Org. Biomol. Chem.* **2009**, *7*, 5084.
(36) Maillard, R. A.; Chistol, G.; Sen, M.; Righini, M.; Tan, J.; Kaiser, C. M.; Hodges, C.; Martin, A.; Bustamante, C. *Cell* **2011**, *145*, 459.
(37) Iosefson, O.; Nager, A. R.; Baker, T. A.; Sauer, R. T. *Nat. Chem. Biol.* **2015**, *11*, 201.
(38) Aubin-Tam, M. E.; Olivares, A. O.; Sauer, R. T.; Baker, T. A.; Lang, M. J. *Cell* **2011**, *145*, 257.
(39) Gersch, M.; Famulla, K.; Dahmen, M.; Göbl, C.; Malik, I.; Richter, K.; Korotkov, V. S.; Sass, P.; Rubsamen-Schaeff, H.; Madl, T.; Brötz-Oesterhelt, H.; Sieber, S. A. *Nat. Commun.* **2015**, *6*, 6320.
(40) Compton, C. L.; Schmitz, K. R.; Sauer, R. T.; Sello, J. K. *ACS Chem. Biol.* **2013**, *8*, 2669.

DOI: 10.1021/jacs.5b03084
J. Am. Chem. Soc. 2015, 137, 8475−8483